Hindawi
Journal of Chemistry
Volume 2018, Article ID 4314969, 14 pages
https://doi.org/10.1155/2018/4314969

Research Article

Photocatalytic Efficiency of TiO_2-Biomass Loaded Mixture for Wastewater Treatment

Devagi Kanakaraju and Soon Pang Wong

Faculty of Resource Science and Technology, Universiti Malaysia Sarawak, 94300 Kota Samarahan, Sarawak, Malaysia

Correspondence should be addressed to Devagi Kanakaraju; kdevagi@unimas.my

Received 15 September 2017; Revised 15 December 2017; Accepted 21 January 2018; Published 20 March 2018

Academic Editor: Davide Vione

Copyright © 2018 Devagi Kanakaraju and Soon Pang Wong. This is an open access article distributed under the Creative Commons Attribution License, which permits unrestricted use, distribution, and reproduction in any medium, provided the original work is properly cited.

The objective of this study was to assess the efficiency of a novel TiO_2/modified sago bark (TiO_2/MSB) mixture for the degradation of sago wastewater effluent by employing response surface methodology (RSM) using chemical oxygen demand (COD) removal as the target parameter. The highest COD removal of 64.92% was obtained using TiO_2/MSB mixture sample prepared by combining 0.2 g/L TiO_2 and 1 w/w% MSB. Given that the highest removal was produced using this mixture sample, further optimisation of sago wastewater treatment was conducted by varying the independent variables, namely, dosage and contact time. Under this optimum condition, 0.10 g of 0.2 g/L TiO_2/1% MSB had successfully reduced 52.83% COD in 120 min. Surface morphology, functional groups, and elemental analysis supported observations of the ability of TiO_2/MSB mixture to remove COD. Additionally, aeration had further improved COD removal by 11%. The regression value ($R^2 > 0.99$) of the model indicated a high degree of correlation between the evaluated parameters. These results proved the feasibility of TiO_2 photocatalysis as an appealing alternative protocol for sago wastewater treatment and solid waste from the industry can be utilised for wastewater degradation.

1. Introduction

Solid or liquid wastes derived from a series of postprocessing steps in the agricultural industry could impose significant environmental impacts if not properly treated or managed. Agro-based industries contribute significantly to the economic growth and development of countries around the globe. Nevertheless, from the environmental point of view, this industry also inevitably tends to increase the accumulation of wastes, which demand considerable attention. The Advanced Oxidation Processes (AOPs) are nonbiological methods that could become the most suitable alternative to degrade organic compounds present in agricultural effluents.

AOPs, which are chemical oxidation processes, have been highly effective in the oxidation of wastewater containing toxic and organic materials [1]. AOPs involve in situ generation of reactive oxygen species (ROS), such as hydroxyl radicals (HO•), O_3, H_2O_2, and superoxide anion radical ($O_2^{\bullet-}$). These ROS act as strong oxidants to oxidise organic compounds into biodegradable forms and simpler end-products, such as CO_2 and H_2O [2, 3]. Among the various AOPs, titanium dioxide (TiO_2) photocatalysis has been known for its potential to effectively treat wastewater. TiO_2 appears to be one of the most widely used photocatalysts because it is biologically and chemically inert, cheap, photostable, and noncorrosive [4]. Nonetheless, the application of TiO_2 in large-scale wastewater treatments is restricted by its limitations. TiO_2 has two major constraints that limit its photocatalytic activity: (i) the large bandgap (3.2 eV for anatase phase) limits its absorption to the UV region, in which only 3 to 5% of the solar spectrum can be utilised for its activation, and (ii) the fast recombination of photogenerated electron-hole pairs occurs during TiO_2 photocatalysis [5]. In addition, nanosized TiO_2 is in the form of slurry (suspension) during treatment, which makes recovery and recycling particularly difficult. Hence, to increase the photocatalytic activity of TiO_2, several methods have been proposed, such as doping with nonmetals and transition metals [6, 7], noble metal or metal ion incorporation [5, 8], fabrication of TiO_2 mixture with other materials [9], surface sensitisation [10], and the inclusion of inert support [11].

TiO_2 was combined with modified sago bark (MSB) to prepare a novel mixture material (TiO_2/MSB), which was then further assessed for the degradation of sago effluent

which is known to be acidic in nature and typically characterised by high COD, biochemical oxygen demand (BOD), and total suspended solids (TSS). The sago residues from sago starch processing mills are abundant and readily available [12]. Sago bark (SB) is a type of solid waste generated during the debarking step of starch extraction process. Deposition or dumping of SB on land is the most common practice among most mill operators to address the disposal problem of this solid waste. Although such practice provides a short-term solution, potential environmental problems could, however, emerge in the long term. To the best of our knowledge, no studies have been performed on sago effluent by means of TiO_2 photocatalysis. SB, the solid waste, was also assessed as a potential support or adsorbent for the preparation of TiO_2-based mixtures. As RSM is known for its superiority in optimising chemical reactions [13], this study applied this statistical tool to determine the optimal conditions for the degradation of sago wastewater effluent, primarily focusing on COD as the target parameter.

Thus, the overall aim of this work was to investigate the effectiveness of the novel material TiO_2/MSB mixture on the degradation of sago wastewater effluent by optimising the process variables, namely, the dosage of TiO_2/MSB mixtures and contact time via RSM.

2. Materials and Methods

2.1. Materials. Ammonium iron(II) sulfate ($Fe(NH_2)_2(SO_4)\cdot 6H_2O$) and potassium dichromate ($K_2Cr_2O_7$) were purchased from R&M Chemical. Silver sulfate (Ag_2SO_4) and mercury(II) sulfate ($HgSO_4$) were obtained from Bendosen. Sulfuric acid (H_2SO_4, 95–97%) and titanium dioxide (TiO_2) (Degussa P25) with a particle size of 20–30 nm were supplied by Merck (Germany). Hydrochloric acid (HCl) and ferroin indicator solution were purchased from J. T. Baker and Sigma-Aldrich, respectively.

2.2. Sago Wastewater. Sago wastewater was collected from Herdsen Sago Industries in Pusa, Sarawak. Sampling was carried out twice. The effluent samples were filled into polyethylene bottles. The bottles were transported to the laboratory and kept refrigerated at 4°C until further analysis. Meanwhile, SB samples were randomly collected from piles of SB, which were produced by the debarking process, and stored in sack bags. The sack bags were also transported to the laboratory for further use. The raw wastewater samples were characterised for water quality parameters, namely, pH, BOD, COD, and TSS. Characteristics of sago wastewater were analysed based on the Standard Methods for Water and Wastewater Examination [14].

2.3. Analytical Determinations. COD, BOD, TSS, and total organic carbon (TOC) analyses were performed based on the Standard Methods for Water and Wastewater Examination [14]. TOC was measured using the OI Analytical (model Aurora 1030) TOC analyser.

2.4. Synthesis of TiO_2 Mixtures (TiO_2/MSB). The sampled SB was washed using distilled water to remove dirt and unwanted materials. The washed SB was dried under sunlight before being cut and ground into a powdered form. The powdered form of SB was sieved to remove unwanted fibre and to obtain particles with similar sizes (500 μm). Subsequently, the powdered form of SB was soaked in 1 M HCl for 1 day. The SB was mainly comprised of cellulose, hemicelluloses, and lignin components [15], which can be dissolved or broken down during a pretreatment process [16]. Mosier et al. [17] and Zheng et al. [18] stated that diluted acid pretreatment process could dissolve almost all hemicelluloses and break down the bonds of cellulose and lignin. Due to the release of soluble organic compounds contained in the plant wastes, the application of untreated plant wastes as adsorbents could lead to several problems, such as low adsorption capacity, and high BOD, COD, and TOC values [19]. The acid-modified SB (MSB) was repeatedly washed using distilled water until the pH became neutral. Then, the neutralised MSB was dried in an oven at 100°C for 2 h. The dried MSB was then mixed with various concentrations of TiO_2 to prepare the TiO_2/MSB mixtures under mechanical stirring.

Figure 1: The prepared TiO_2/MSB mixture.

TiO_2 concentration was varied from 0.2 to 0.8 g/L, while the weight percentage of MSB was fixed as either 1 w/w% or 3 w/w%. A total of six TiO_2/MSB mixtures were prepared: (i) 0.2 g/L TiO_2/1% MSB, (ii) 0.2 g/L TiO_2/3% MSB, (iii) 0.4 g/L TiO_2/1% MSB, (iv) 0.4 g/L TiO_2/3% MSB, (v) 0.8 g/L TiO_2/1% MSB, and (vi) 0.8 g/L TiO_2/3% MSB. In this study, a fixed concentration of TiO_2 was added to a fixed weight percentage of MSB in a beaker, followed by 100 mL of ultrapure water. The mixture was then stirred at 750 rpm for 1 to 2 h to attain a homogeneous suspension. Next, the suspension was filtered and dried in an oven at 100°C for 2 h. The dried TiO_2/MSB mixture was pounded into a powdered form for further analysis. Figure 1 shows the prepared TiO_2/MSB mixture.

2.5. Material Characterisations. The raw SB, MSB, and TiO_2 mixtures were characterised for their surface morphology using a scanning electron microscope (SEM) (model: JOEL JSM-6390LA). The functional groups of TiO_2, MSB, and TiO_2/MSB were identified using Fourier transform infrared spectroscopy (model: Thermo Nicolet iS10). Elemental analysis of TiO_2/MSB was conducted using energy-dispersive X-ray spectroscopy (EDX) (model: JOEL JSM-6390LA). The crystalline structures of the mixture were

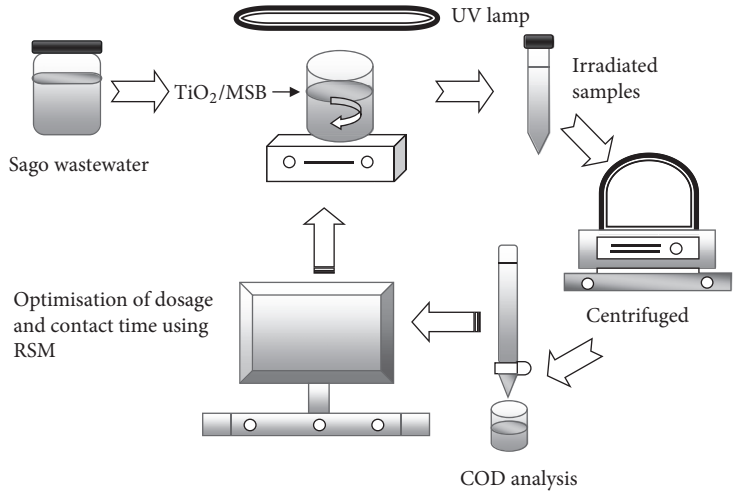

Figure 2: Schematic diagram of a lab-scale TiO_2 photocatalytic experiment using TiO_2/MSB mixture.

observed using X-ray diffraction (XRD, PANalytical X'pert Pro) method with Cu Kα radiation (λ = 0.154 nm) in the scanning range of 2θ between 10° and 80°, at a rate of 0.04° per second. For phase identification, an automatic JCPDS library search and match was used.

2.6. Photocatalytic Experiment. For the photocatalytic experiment, the dosage of TiO_2/MSB mixture and contact time were optimised by employing the RSM. Different dosages of TiO_2/MSB mixture were added to a beaker containing 200 mL of filtered sago wastewater sample. Sago wastewater sample was filtered prior to treatment to ensure that the roughage, being the major portion of the wastewater, does not interfere with the final COD reading and block the penetration of UV light during the photocatalytic experiment. The solution mixture was subsequently stirred at 750 rpm in the dark for 30 min to establish absorption and equilibrium by the TiO_2/MSB mixture. The mixture was then irradiated using a UVC lamp (λ = 254 nm, Phillips TUV 8 W) for 2 h under continuous stirring (Figure 2). The distance of the vertically placed UV lamp from the solution beaker was fixed at 9 cm. Temperature and light intensity were measured during all photocatalytic experiments. A light meter (Sunche, HS1010) was used to measure the amount of light emitted by the UV lamp. Temperature of the solution mixture in the beaker ranged from 32°C to 34°C while the light intensity varied between 128 and 135 lux. Samples were withdrawn using a syringe prior to irradiation (after 30 min equilibrium) and at fixed time intervals throughout the 2 h irradiation period. The collected samples were centrifuged and the supernatant was subjected to COD analysis.

2.7. Experimental Design. The present study also used the central composite design (CCD). CCD consists of 2^k factorial points, augmented with 2^k axial points and a centre point, where k represents the number of variables involved [2]. In the present work, the independent variables were TiO_2/MSB mixture dosage and contact time, while COD removal was the dependent variable (response). A total of 13 experiments were conducted with 4 factorial points, 4 axial points, and 1 centre point. The centre point was repeated five times to obtain an accurate result. Table 1 shows the ranges and levels of the independent variables in coded units.

The initial design included 13 tests, based on a CCD, as shown in [20]

$$\eta\,(\%) = \frac{\mathrm{COD}_0 - \mathrm{COD}_f}{\mathrm{COD}_0} \times 100, \tag{1}$$

where η represents the percentage of COD removal, while COD_0 and COD_f represent the measured COD values, before and after the TiO_2 photocatalytic experiment, respectively. Table 2 lists the 13 experiments conducted in this study, with the ranges and levels in coded units.

The Design-Expert 7.1.6 software was used to analyse the experimental data that were fitted to a second-order polynomial equation. The interaction between the dependent and independent variables was attained through the following equation [21]:

$$\eta = \beta_0 + \sum_{i=1}^{k} \beta_i x_i + \sum_{i=1}^{k} \beta_{ii} x_i^2 + \sum_{i=1}^{k} \sum_{j=1}^{k} \beta_{ij} x_i x_j + \varepsilon, \tag{2}$$

where η represents the predicted response (dependent variable); k is the number of patterns; i and j are the index numbers for the patterns; β_0 is the offset or free term, known as the intercept term; $x_1, x_2, \ldots, x_k$ are the coded independent variables; β_i is the first-order (linear) main effect; β_{ii} is the quadratic (square) effect; β_{ij} is the interaction effect; and ε is the random error between the experimental and predicted values.

By representing (2) with two independent variables, it could be simplified as shown in

$$\eta = \beta_0 + \beta_1 X_1 + \beta_2 X_2 + \beta_3 X_1^2 + \beta_4 X_2^2 + \beta_5 X_1 X_2. \tag{3}$$

Due to the regression and mean square residual error, analysis of variance (ANOVA) was used to test the statistical

Table 1: Ranges and levels of the independent variables for RSM.

Variables	Coded	Ranges and levels				
		$-\alpha$	-1	0	1	$+\alpha$
Dosage (g)	X_1	0.06	0.10	0.20	0.30	0.34
Contact time (min)	X_2	11.36	30.00	75.00	120.00	138.64

Table 2: RSM for the two independent variables in corresponding natural values and coded units.

Run	Independent variables		Coded variables	
	Dosage (g)	Contact time (min)	X_1	X_2
(1)	0.20	75.00	0	0
(2)	0.20	11.36	0	$-\alpha$
(3)	0.30	30.00	1	-1
(4)	0.20	75.00	0	0
(5)	0.30	120.00	1	1
(6)	0.34	75.00	$+\alpha$	0
(7)	0.10	30.00	-1	-1
(8)	0.06	75.00	$-\alpha$	0
(9)	0.20	75.00	0	0
(10)	0.20	75.00	0	0
(11)	0.20	138.64	0	$+\alpha$
(12)	0.20	75.00	0	0
(13)	0.10	120.00	-1	1

significance of the ratio of mean square variation [22]. The coefficient of determination (R^2) was used to express the quality of the fit of the polynomial model. Meanwhile, the probability values (p values) with 95% confidence level can act as a tool to evaluate the significance of the model terms [23]. Generally, if the significant probability value ($p > F$) is small (<0.05) and the p value is less than 0.01, the model is considered to be statistically significant and acceptable [24]. The main indicators, which included the probability value (Prob. > F), model F-value (Fisher's variation ratio), and adequate precision, showed the adequacy and significance of the employed model. To find an optimum condition, response plots, namely, contour and 3D plots, were used. Fischer's F-test was utilised to determine the statistical significance and to optimise the desired target fixed for maximum removal of COD. For process optimisation, the desired target for the response (COD removal) was selected as "target," while the independent variables (dosage and contact time) were chosen to be "within the range." To determine the best and optimised local maximum, these individual targets were combined into an overall desirability function by the software [25].

3. Results and Discussion

3.1. Characterisation of TiO_2/MSB Mixture. Surface morphologies of raw SB and MSB acquired by SEM are shown in Figures 3(a) and 3(b), respectively. SEM micrographs revealed that the chemical modification by HCl has afforded a rougher surface morphology for the MSB (Figure 3(b)) compared to the unmodified SB (Figure 3(a)). Figure 3(a) shows the presence of fibre or starch granules (white arrow) on the surface of SB, which appeared to decrease or almost disappeared in the SEM micrograph of MSB (Figure 3(b)). The average pore sizes of raw SB and MSB were 0.08 μm and 0.10 μm, respectively. As the pore size difference between the raw SB and MSB was marginal, this could imply that the HCl treatment did not alter the pore size of SB.

SEM images of 0.2 g/L TiO_2/1% MSB mixture, before and after photocatalytic treatments, are shown in Figures 4(a) and 4(b), respectively. Figure 4(a) clearly shows that TiO_2 particles (white circle) have been successfully attached on the surface of the MSB (white arrow). The average pore size of TiO_2/MSB was recorded as 0.16 μm. However, in Figure 4(b), the amount of TiO_2 particles attached on the MSB surface was observed to be reduced after undergoing photocatalytic treatment. This could be due to the fall of TiO_2 from the MSB during the photoinduced degradation of organic pollutants present in sago effluent, as TiO_2/MSB mixture was synthesised via mechanical stirring [26]. As such, TiO_2/MSB could not potentially be recycled. Furthermore, no pores were detected after the treatment (Figure 4(b)). A possible explanation is that this might be due to the adsorption of organic pollutants on the adsorbent's pores.

The EDX spectrum of the optimum TiO_2/MSB mixture that consisted of 0.2 g/L TiO_2/1% MSB is shown in Figure 5. The presence of three main elements, namely, C, Ti, and O, in the mixture was detected and their mass percentages are summarised in Table 3. As shown in the table, the mass percentages of C, Ti, and O were found to be 14.59%, 26.53%, and 58.88%, respectively. The presence of Ti and O indicated that the TiO_2/MSB mixture has been successfully prepared in this study.

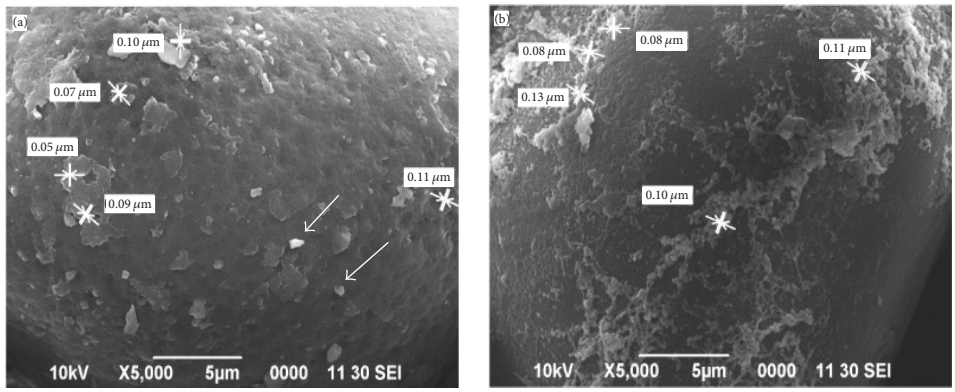

(a) (b)

Figure 3: SEM micrographs for (a) raw sago bark (SB) and (b) modified sago bark (MSB).

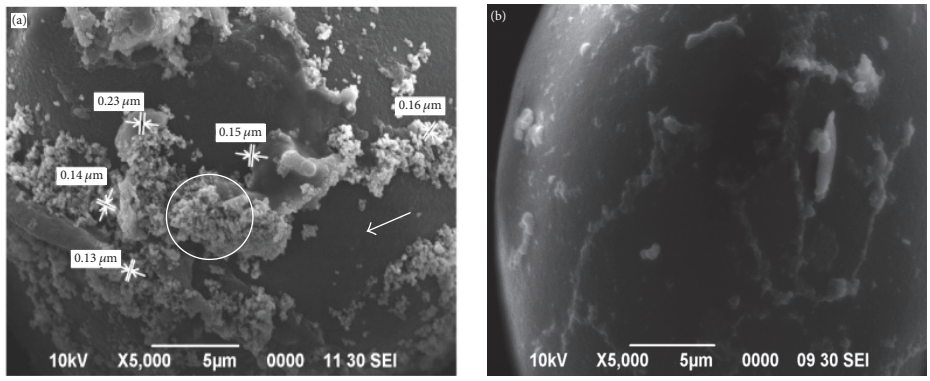

(a) (b)

Figure 4: SEM micrographs of 0.2 g/L TiO_2/1% MSB mixture: (a) before treatment and (b) after treatment.

Table 3: Mass percentage of elements in 0.2 g/L TiO_2/1% MSB mixture.

Elements	Mass percentage (%)
C	14.59
O	26.53
Ti	58.88
Total	100.00

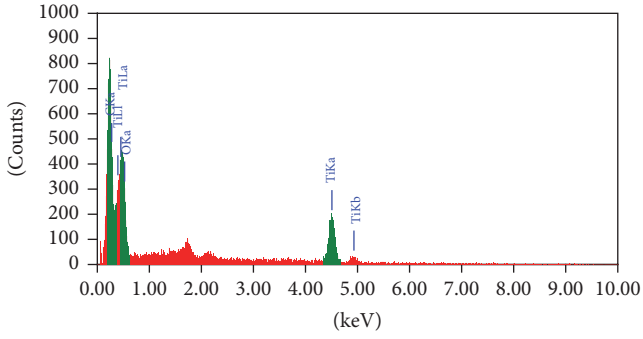

Figure 5: EDX data of 0.2 g/L TiO_2/1% MSB mixture.

The FTIR spectra of commercial TiO_2, MSB, and 0.2 g/L TiO_2/1% MSB mixture in the range of 4000 to 400 cm^{-1} wavenumber are shown in Figure 6. The region between 400 and 700 cm^{-1} in Figure 6(a) was assigned to Ti-O stretching and Ti-O-Ti bridging stretching modes [27]. The presence of TiO_2 was confirmed by the peaks at 526.97 cm^{-1} and 666.97 cm^{-1} (Figure 6(a)). The peaks located at 3352.77 cm^{-1} and 3326.24 cm^{-1} in Figures 6(b) and 6(c), respectively, corresponded to the stretching vibrations of hydroxyl groups (OH) present in the cellulose, hemicelluloses, and lignin of SB [28]. The peak around 2928 cm^{-1} in both Figures 6(b) and 6(c) corresponded to the C–H stretching vibrations in the methyl, methoxyl, and methylene groups, which were present in the saccharide and aromatic structures of the hydrolysed products [29]. The strong stretching vibration peak observed around 1643 cm^{-1} (Figures 6(b) and 6(c)) can be attributed to a carbonyl group (C=O), which provides evidence of the high carbon content in SB [30]. As shown in Figure 6(c), the peaks at 1425.97 cm^{-1} and 1368.15 cm^{-1} represent the CH_2 and OH bending, respectively [28]. The peaks around 1155 cm^{-1} and 1020 cm^{-1} confirmed the presence of arabinosyl residues and α-glucan of hemicellulose, respectively [30]. The peak at

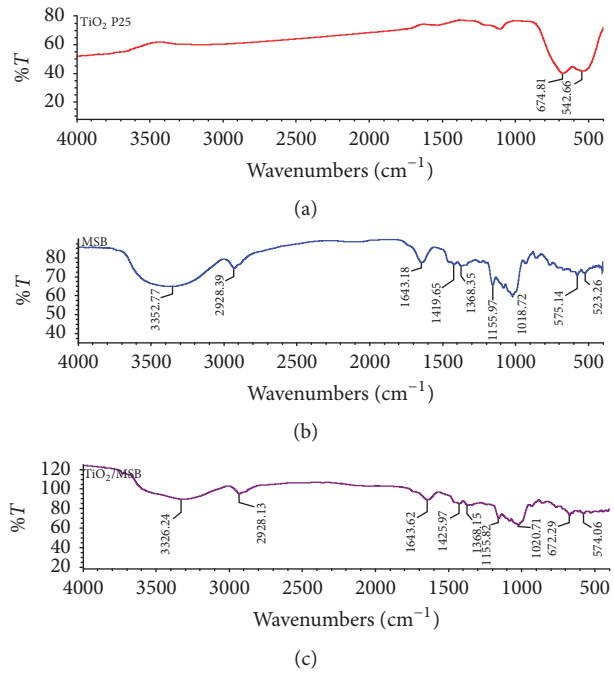

FIGURE 6: FTIR spectra of (a) TiO_2, (b) MSB, and (c) 0.2 g/L TiO_2/1% MSB mixture.

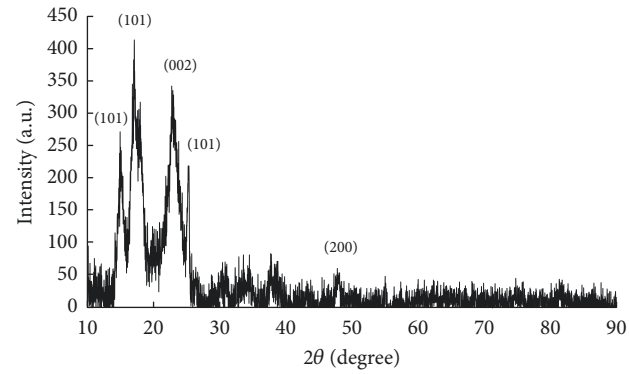

FIGURE 7: XRD pattern of 0.2 g/L TiO_2/1% MSB mixture.

672.29 cm^{-1} indicated the presence of TiO_2 in the TiO_2/MSB mixture (Figure 6(c)), which was found to be absent in the MSB spectrum (Figure 6(b)). Furthermore, the appearance of absorption peaks around 575 cm^{-1} in both Figures 6(b) and 6(c) can be associated with the accumulation of oxide particles in SB [30].

Figure 7 shows the XRD pattern of 0.2 g/L TiO_2/1% MSB mixture. Five of the diffraction peaks centered at 2θ = 15.03° (101), 17.01° (101), 22.82° (002), 25.33° (101), and 47.92° (200) corresponded to 0.2 g/L TiO_2/1% MSB mixture. As shown in Figure 7, the diffraction peaks located at 2θ values of 25.33° and 47.92° corresponded to the (101) and (200) anatase TiO_2 crystal planes, respectively [31]. The peaks at 15.03° (101), 17.01° (101), and 22.82° (002) in Figure 7 corresponded to cellulose. Abou-Sekkina et al. [32] reported the XRD pattern of cellulose for an untreated fibre with the crystalline peaks at 2θ values of 15.0° (101), 16.5° (101), and 22.8° (002), respectively. The obtained XRD pattern indicated that HCl pretreatment did not completely remove the cellulose or hemicelluloses in MSB.

3.2. Photodegradation of Wastewater. The supernatant of sago effluent appeared as pale brownish in colour, with a pungent smell. The sago wastewater had also demonstrated an acidic value ranging from 5.12 to 6.06. The TSS, BOD, and COD of the wastewater ranged from 4,000 to 8,200 mg/L, 800 to 3,300 mg/L, and 6,192 to 34,048 mg/L, respectively. Several preliminary experiments were conducted in the presence of UV irradiation using (i) sago wastewater only, (ii) a mixture of SB and sago wastewater, (iii) a mixture of MSB and sago wastewater, and (iii) a mixture of sago wastewater and TiO_2. Sago wastewater was treated under UV irradiation to investigate the effect of photolysis, while the degradation of sago wastewater in the presence of commercial TiO_2, SB, and MSB was performed to assess their individual effects on the degradation of organic pollutants. The photolysis of sago wastewater under UV irradiation exhibited poor COD removal of less than 10% after 120 min of treatment (Figure 8). This thus confirmed the poor photolysis effect on the degradation of sago wastewater. On the other hand, the photocatalytic treatment of sago wastewater in the presence of 0.50 g/L TiO_2 yielded much better COD removal. The highest COD removal of 45.00% was attained after 90 min of UV irradiation using 0.50 g/L TiO_2. This value was slightly higher compared to the value obtained in the presence of SB and MSB, with 24.24% and 37.90%, respectively, after 120 min of treatment. The higher removal percentage of COD by the MSB could be due to the adsorption effect demonstrated by the modified material. TiO_2 photocatalysis has thus ascertained its contribution in removing organic pollutants from sago wastewater, despite the slight fluctuation observed during treatment (Figure 7). This could be due to the solution's opacity, which could have increased the light scattering effect of the TiO_2 nanoparticles used in the treatment [33]. The solution's opacity, caused in part by TiO_2 nanoparticles [34], would lead to a reduction of light penetration in the wastewater solution [35]. Moreover, interactions between the pollutants and the intermediates or degradants formed during the course of treatment could have plausibly caused the TiO_2 particles to coagulate, leading to a reduction of TiO_2 surface area and consequently its photocatalytic efficiency [36].

Six different TiO_2/MSB mixtures, which were prepared under different conditions, were applied in the sago wastewater degradation (Figure 9). The concentration of TiO_2 was varied from 0.20 g/L to 0.80 g/L, while the amount of MSB was fixed as either 1 w/w% or 3 w/w%. Among these samples, both 1 w/w% and 3 w/w% of MSB, when combined with 0.2 g/L TiO_2, had yielded relatively high COD removal of 64.29% and 61.54%, respectively, after 120 min of treatment. The obtained percentages of COD removal by the four other mixtures under similar treatment time had varied from 7.69% to 56.52%. The higher COD lowering capacity exhibited by TiO_2/MSB mixtures compared to the results obtained using only the commercial TiO_2 and MSB (Figure 9) could

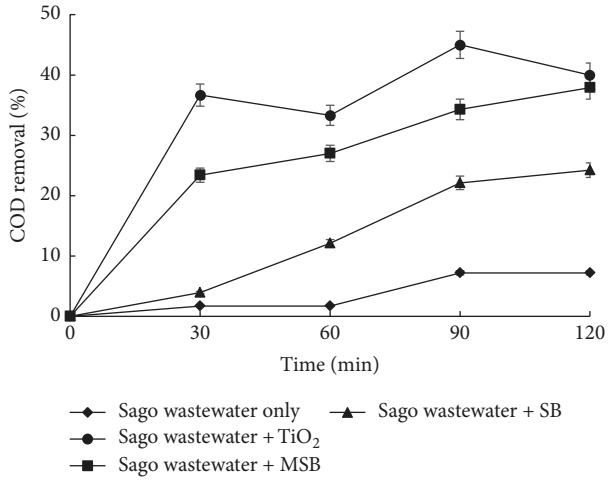

Figure 8: Photodegradation of sago wastewater under different conditions (experimental conditions: 0.5 g/L TiO_2; 0.5 g/L SB; 0.5 g/L MSB).

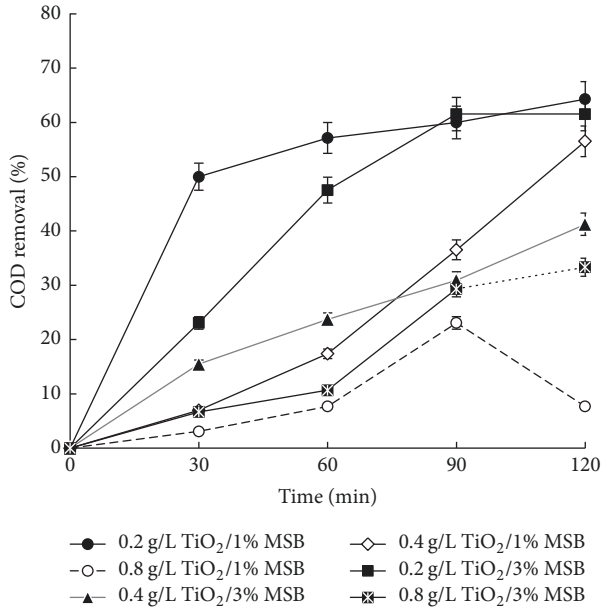

Figure 9: Photocatalytic experiments using various TiO_2/MSB mixtures.

be attributed to the synergistic effect between TiO_2 and MSB. The presence of the synergistic effect in the TiO_2/MSB mixtures could probably be linked to its dual effects, namely, adsorption and degradation. TiO_2 has been reported to be highly favourable in photocatalytic treatments [37]. Meanwhile, the MSB could have acted as an adsorbent in the fabricated TiO_2/MSB mixtures to improve the affinity of TiO_2 towards the organic pollutants [38]. Ngamsopasiriskun et al. [11] reported that TiO_2/commercial activated carbon (AC) showed a synergistic effect between TiO_2 and AC in achieving 68.03% of phenol degradation after 4 h of treatment. As the 0.2 g/L TiO_2/1% MSB mixture was considered as an optimum mixture based on the obtained percentage of COD removal, this mixture was chosen to further investigate sago wastewater degradation by varying two other parameters, namely, dosage and contact time via RSM study.

3.3. Model Fitting. Based on the CCD, 13 sets of experiments with different operating conditions were conducted to investigate the effects of the independent variables (dosage of TiO_2/MSB mixture and contact time) in the photocatalytic treatment of sago wastewater (Table 2). The experimental response (η), which is the percentage of COD removal, was chosen to determine the optimal conditions for the independent variables, which may affect the efficiency of the photocatalytic treatment. The complete 13 sets of experimental design matrices and responses based on the experimental results and predicted values of COD removal proposed by CCD are tabulated in Table 4. The resulting second-order polynomial equation was generated and the equation, in terms of the coded factors, is shown as

$$\eta\,(\%) = 20.68 - 13.72X_1 + 5.00X_2 - 3.42X_1X_2 + 7.84{X_1}^2 + 1.68{X_2}^2. \quad (4)$$

As shown in Table 4, the obtained percentage of COD removal efficiencies varied from 14.90% to 55.78% and the predicted values from the model matched these experimental

Table 4: Experimental results and predicted values of η for the percentage of COD removal using RSM.

Run	COD removal, η (%)	
	Experimental results	Predicted values
(1)	19.49	20.68
(2)	16.77	16.97
(3)	15.14	14.90
(4)	21.43	20.68
(5)	18.40	18.06
(6)	16.67	16.96
(7)	35.71	35.52
(8)	55.55	55.78
(9)	21.26	20.68
(10)	20.41	20.68
(11)	30.77	31.10
(12)	20.83	20.68
(13)	52.63	52.34

results satisfactorily, as seen in Figure 10. The figure also depicts a regression coefficient (R^2) value of 0.99, which confirmed the reasonably good agreement between the experimental and predicted values. The slope for Figure 10 was 0.9997. Therefore, the developed model is suitable to predict COD removal in sago wastewater treatment.

3.4. Statistical Analysis. ANOVA is defined as a statistical technique that subdivides the total variation in a set of data into component parts related to specific variation sources to test the hypotheses on the parameters of the model [39]. Due to the regression and mean square residual error, ANOVA was used to determine the statistical significance of the ratio

Table 5: ANOVA for the percentage of COD removal.

Source	Sum of squares	Degrees of freedom (df)	Mean square	F value	p value Prob. > F
Model	2,184.41	5	436.68	1,019.22	<0.0001
X_1	1,506.97	1	1,506.97	3,515.66	<0.0001
X_2	199.79	1	199.79	466.10	<0.0001
X_1X_2	46.65	1	46.65	108.83	<0.0001
X_1^2	427.98	1	427.98	998.45	<0.0001
X_2^2	19.54	1	19.54	45.59	0.0003
Residual	3.00	7	0.43		
Lack of fit	0.59	3	0.20	0.33	0.8076
Pure error	2.41	4	0.60		
Cor. total	2,187.41	12			

R^2 = 0.9986; adj. R^2 = 0.9976; pred. R^2 = 0.9964; adeq. precision = 91.919; CV = 2.47%.

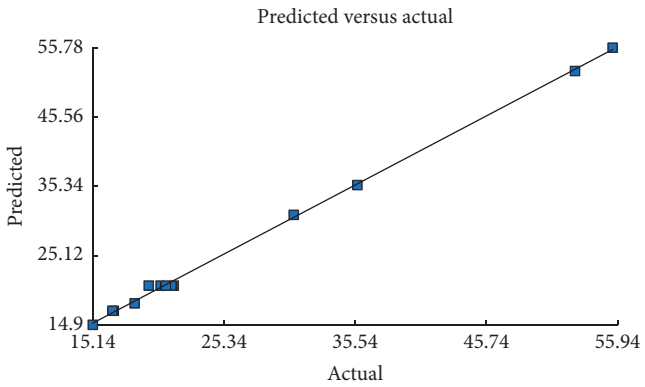

Figure 10: The scatter plot of the predicted versus experimental values for COD removal (%) (R^2 = 0.99).

of mean square variation. Table 5 shows the ANOVA results for the second-order equation used to fit the COD removal from sago wastewater. As shown in the table, the F-values were high for all regressions. The large F-values indicated that most of the variations in the responses can be interpreted by the regression equation.

The ANOVA results for COD removal from sago wastewater using TiO_2/MSB mixture produced an F-value of 1,019.22 for the quadratic model, indicating that the model is significant. The "Prob. > F" (<0.0001) for the second-order polynomial fitting implied that the model terms were significant at 95% probability level. The adequacy of the model was tested via the "lack-of-fit F-tests" [40]. The "lack of fit F-value" of 0.33 implied that the lack of fit was not significant, relative to the pure error. There was an 80.76% chance that a "lack-of-fit F-value" could occur due to noise. The insignificant "lack of fit" demonstrated that the model is adequate. The ANOVA results for the COD removal (η) showed a significant ($P < 0.05$) response surface model with high R^2 value of 0.9986. The adjusted R^2 value of 0.9976 and predicted R^2 value of 0.9964 were found to be at the maximum, indicating that the quadratic model provided an excellent interpretation of the relationship between the independent variables and the corresponding response. Adequate (adeq.) precision measures the signal-to-noise ratio or, in other words, is a measure of the range in predicted response relative to its associated error. The desired ratio of adequate precision is >4 [41]. The adequate precision ratio of 91.919 showed an adequate signal (Table 5). Hence, based on the ANOVA results, this quadratic model (see (3)) could be used to navigate the design space. Low coefficient of variance (CV) value of 2.47% emphasised the good precision and reliability of the experiments. It is known that the greater the value of CV, the lower or poorer the reliability of the experiment [42].

3.4.1. Effect of Dosage and Contact Time on COD Removal Percentage. The three-dimensional (3D) response surface and the two-dimensional (2D) contour plots of the model-predicted responses were obtained using the Design-Expert software. From these plots, two variables that vary within the experimental ranges were plotted and utilised to assess the interactive relationships between the variables and the response for TiO_2 photocatalysis of sago wastewater.

Figures 11(a) and 11(b) illustrate the 3D surface and 2D plot of the polynomial model, respectively, for COD removal, with respect to the dosage of TiO_2/MSB mixture and contact time during the photocatalytic treatment. The obtained 3D surface plot depicts that the highest COD removal of 52.63% would be achieved in 120 min using 0.10 g of TiO_2/MSB mixture (Figure 11(a)). It is evident that COD removal increased with increasing contact time for each TiO_2/MSB mixture dosage investigated (0.10 g to 0.30 g). A low dosage of 0.10 g demonstrated a significant increase in the COD removal as the contact time increased, which was different from the trend observed for the high dosage of 0.30 g (Figure 11(a)). In the case of photoreaction over high dosage of TiO_2/MSB mixture, the intermediates or degradation products that remained in the suspension could still be structurally similar to the initial organic compounds. Their concentrations and photostability might also differ depending on the applied dosage. The applied contact time might be too short to achieve complete oxidation [43].

On the other hand, the percentage of COD removal declined at the tested contact times (30–120 min) when the dosage of TiO_2/MSB mixture was increased from 0.10 g to 0.30 g (Figure 11(a)). The lowest COD removal of 15.14% was attained at 30 min using the highest dosage of TiO_2/MSB

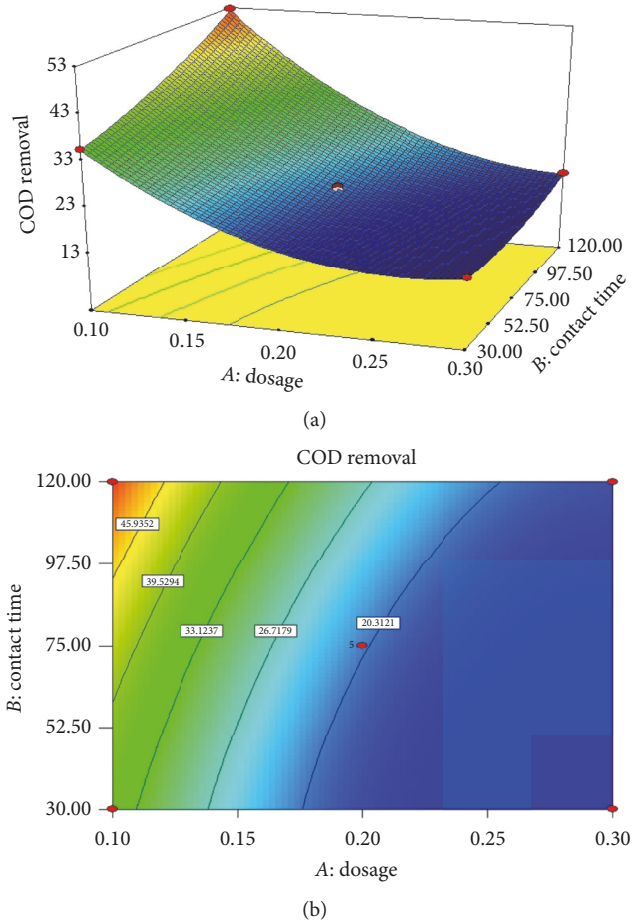

Figure 11: Interaction between dosage and contact time on COD removal: (a) 3D surface and (b) contour plot of the response surface curve.

mixture, 0.30 g. COD removal, however, remained almost constant despite an increase in the contact time from 30 min to 120 min. The reduction of COD removal at a higher dosage of TiO_2/MSB mixture could be explained by several facts. An increased level of suspension turbidity as a result of excessive photocatalyst dosage could block the UV irradiation required for the catalyst activation [44]. Hence, it is crucial to optimise the dosage of TiO_2/MSB mixture and contact time to maximise COD removal in sago wastewater.

3.5. The Proposed Mechanism of TiO_2/MSB Photocatalytic Degradation. Typically, the photocatalytic degradation process involves three steps: (1) adsorption of organic pollutant on the TiO_2 surface, (2) surface photodegradation of organic pollutant, and (3) final product desorption from the TiO_2 surface [9, 45]. In the TiO_2/MSB photocatalytic oxidation process, the reaction was activated by the absorption of photons with sufficient energy corresponding to the bandgap energy of the photocatalyst, TiO_2. Upon UV irradiation, TiO_2 particles on the MSB surface will interact with UV light to promote an electron (e^-) from the valence band to the conduction band, thus generating a positive hole (h^+) in the valence band (see (5)). The pertaining reactions at the TiO_2 surface, which govern the degradation of organic pollutants, are expressed by the following equations [44]:

$$TiO_2 \xrightarrow[254\,\text{nm}]{h\nu} TiO_2\left(e^-_{CB} + h^+_{VB}\right) \quad (5)$$

$$TiO_2\left(h^+_{VB}\right) + H_2O \longrightarrow TiO_2 + H^+ + \bullet OH \quad (6)$$

$$TiO_2\left(h^+_{VB}\right) + OH^- \longrightarrow TiO_2 + \bullet OH \quad (7)$$

$$TiO_2\left(e^-_{CB}\right) + O_2 \longrightarrow TiO_2 + O_2^{\bullet -} \quad (8)$$

$$R\text{-}H + \bullet OH \longrightarrow R\bullet^+ + H_2O \quad (9)$$

$$R\left(h^+_{VB}\right) + H_2O \longrightarrow R\bullet^+ \longrightarrow \frac{\text{Intermediates}}{\text{final degradation products}} \quad (10)$$

where R/R-H is the pollutant molecule and $h\nu$ is the photon energy required to excite the electron from the valence band (VB) to the conduction band (CB). Since MSB acts as an adsorbent, it is anticipated that the accumulated pollutants and intermediates on its surface will be oxidised by the photoactivated TiO_2 into simpler products, such as CO_2, H_2O, and other degradation products (see (10)). Figure 12 illustrates the proposed photoinduced mineralisation of organic pollutants using TiO_2/MSB mixture. The synergistic effects, adsorption, and photocatalysis exhibited by TiO_2/MSB mixture would aid the degradation of organic pollutants in sago effluent.

3.6. Kinetic Evaluation. The kinetics of COD degradation for sago wastewater were analysed using the first-order model as expressed in [46]

$$\ln\left(\frac{C_0}{C_t}\right) = k_{app}t, \quad (11)$$

where k_{app} represents the apparent rate constant of the first-order reaction (min^{-1}), C_0 is the equilibrium COD of sago wastewater after adsorption in the dark, and C_t represents the remaining COD of sago wastewater at fixed irradiation time interval. Table 6 shows the kinetics of COD degradation for sago wastewater during different treatments performed. The highest rate constants produced by 0.2 g/L TiO_2/1% MSB mixture confirmed the synergistic effects of adsorption and photocatalysis compared to the individual effects of SB, MSB, and TiO_2.

3.7. Optimisation Analysis and Verification of the Results. The optimisation process was performed using RSM, with the objective of identifying the optimum conditions for TiO_2/MSB photocatalysis, which were to minimise the usage of TiO_2/MSB and to reduce the contact time. The optimisation process was conducted by verifying the desired target for each of the variables and responses. Thus, the process variables, namely, the dosage of TiO_2/MSB and the contact time, were chosen to be "in range," while a "target" was declared as the desired target for the COD removal to

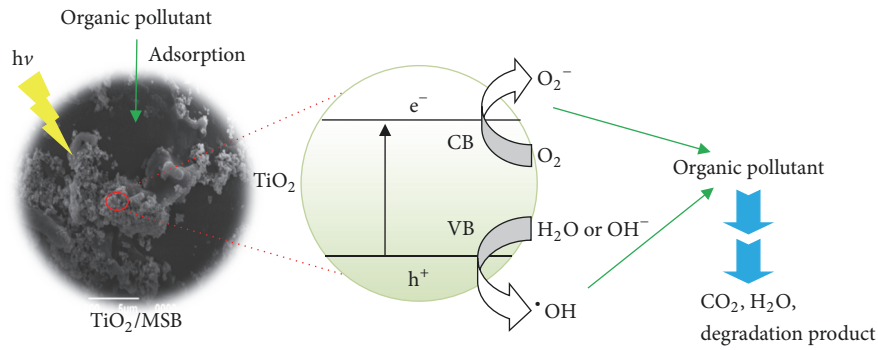

Figure 12: Schematic illustration of the adsorption and photocatalytic degradation of organic pollutants by TiO_2/MSB mixture.

Table 6: Kinetics of COD degradation for sago wastewater during different treatments.

Treatment	k_{app} value (min^{-1})	R^2 value
Sago wastewater only	0.0007	0.86
Sago wastewater + SB	0.0026	0.96
Sago wastewater + MSB	0.0037	0.90
Sago wastewater + TiO_2	0.0039	0.63
Sago wastewater + 0.2 g/L TiO_2/1% MSB	0.0076	0.80

Table 7: Optimum values of the parameters for TiO_2 photocatalysis for maximum efficiency.

Parameter	Optimum value
COD removal, Y (%)	52.34
Dosage (g)	0.10
Contact time (min)	120

Table 8: Experimental and predicted values for COD removal under the optimum conditions.

Type of value	COD removal (%)
Experimental	52.83
Predicted	52.34

achieve the highest performance. Table 7 lists the optimum conditions derived from the statistical software.

As shown in Table 7, it has been predicted that 52.34% of COD can be removed by means of photocatalytic treatment under optimum TiO_2/MSB dosage and contact time of 0.10 g and 120 min, respectively. A series of experiments were conducted to validate the predicted response from the optimisation process. Average percentage removal of COD of 52.83% was achieved from the duplicate experiments. The effective stirring of the treatment solution may have maintained sufficient oxygen level and also contributed to the obtained COD removal. Table 8 compares the efficiency of the experimental and predicted COD removal under the established optimum conditions. The actual experimental values of COD removal were only marginally different from the predicted values. The validity of the developed polynomial model was thus verified for the photocatalytic removal of COD using the fabricated mixture material.

Under the optimum conditions, the COD of the treated sago wastewater was reduced from the initial value of 2,956.80 mg/L to 1,056.00 mg/L after 120 min of treatment (Figure 13). The COD result revealed that the TiO_2/MSB mixture was effective in reducing the COD level in sago wastewater. However, the TOC level of the treated sago wastewater had demonstrated an increase from 850.00 mg/L to 1,050.00 mg/L during the first 60 min and was reduced to 900.00 mg/L after 120 min (Figure 13). The presence of soluble organic compounds, such as hemicelluloses and lignin, in the SB, which were not fully removed during the acid pretreatment, could have contributed to the increase of TOC level [19]. Thus, the increase of TOC might be due to the leaching of organic materials from the MSB. It was also notable that the initial TOC and the final TOC levels showed no significant difference despite the changes observed, as previously explained (Figure 13). This thus implies that a more stringent oxidising condition and a longer reaction time might be needed to significantly reduce the TOC level due to the presence of intermediates and degradation products with differing nature [47]. Generally, the COD value can be considered to be more accurate in the determination of wastewater treatment efficiency compared to the TOC level [48]. COD measures the oxygen required to oxidise the organic compounds in wastewater, while TOC measures the amount of carbon in wastewater, including dissolved CO_2 and carbon compounds, such as amine and aromatic compounds [47]. The final COD obtained revealed that the sago wastewater was less suitable to be discharged into the river as the law requirement for COD is 200 mg/L [49]. Future studies will be performed to improve the applied treatment to produce an effluent that fits the required value.

3.8. Comparison of TiO_2 Photocatalysis under Different Conditions. The presence of O_2 is known to enhance the degradation of wastewater in the TiO_2 photocatalytic treatment as it can inhibit the recombination of electron-hole pairs and produces more HO• radicals during photocatalysis [50]. Experiments were performed to investigate the effect of O_2 on the degradation of sago wastewater using the optimised TiO_2/MSB mixture. An air diffuser was used to continuously supply aeration during the photocatalytic treatment. Raw SB

(without chemical modification) was also used to prepare TiO_2/SB mixture, in the same way as the optimised 0.2 g/L TiO_2/1% MSB mixture. Figure 14 shows the percentage of COD removal achieved under different conditions. Under the aerated condition, COD removal was observed to positively increase to 63.89% compared to the 52.83% under nonaerated condition using the same TiO_2/MSB mixture. Aljuboury et al. [44] reported that the presence of air bubbling as a source of oxygen had markedly increased the degradation rate of COD in petroleum wastewater by 12%. A maximum 76% of COD removal was also achieved using TiO_2/ZnO/air system [44].

The role of O_2 in photocatalysis includes being an electron acceptor, getting involved in the formation of other oxidative species (e.g., hydroxyl radical, superoxide radical, and hydrogen peroxide), and preventing reduction reactions [51]. O_2 can also act as electron scavenger to prevent the recombination of photogenerated electron-hole pairs, which could reduce the photocatalytic activity of TiO_2/MSB [3, 34]. The photogenerated electrons (e^-_{CB}) scavenged by the adsorbed molecular oxygen on the TiO_2/MSB surfaces produce •OH radicals as shown in (12) and (13) [52]

$$e^-_{CB} + O_2 \longrightarrow O_2^{\bullet -} \quad (12)$$

$$O_2^{\bullet -} + H^+ \longrightarrow HO_2^{\bullet} \quad (13)$$

The $\bullet O_2H$ radical can further generate H_2O_2 (see (14)) and, subsequently, HO• radicals (see (14)–(17)), thus preventing the recombination of electron-hole pairs, which are known to cause low TiO_2 photocatalytic quantum yield.

$$HO_2^{\bullet} + HO_2^{\bullet} \longrightarrow H_2O_2 + O_2 \quad (14)$$

$$H_2O_2 + e^-_{CB} \longrightarrow \bullet OH + OH^- \quad (15)$$

$$H_2O_2 + O_2^{\bullet -} \longrightarrow \bullet OH + OH^- + O_2 \quad (16)$$

$$H_2O_2 \xrightarrow{h\nu} 2HO^{\bullet} \quad (17)$$

When the recombination rate of photogenerated electron-hole pairs is reduced, positive holes can either directly oxidise the organic pollutants or react with OH^- anions to form powerful HO• radicals. This would aid and promote the reduction of COD because more organic material in the sago effluent can be oxidised to its simpler form. Hence, COD level in sago effluent can be reduced by supplying O_2 via aeration, which is an economical way for continuously supplying O_2 to enhance the TiO_2 photocatalytic treatment of sago effluent. Additionally, operating costs can be reduced if air is used instead of pure oxygen in pilot scale treatments [34].

Another TiO_2 mixture, which was prepared using raw SB as an adsorbent, had yielded only 43.75% COD removal. This finding appeared consistent with those obtained by Acar and Eren [53], whereby acid-treated poplar sawdust (a plant waste) had produced appreciably better removal of Cu^{2+} at 92.38%, compared to the untreated sample, which had only removed 47.05% of Cu^{2+}. It was reported that the improved adsorption efficiency exhibited by the acid-treated poplar sawdust had contributed to the increased percentage of Cu^{2+} removal. Limitations arising from the usage of untreated plant wastes as adsorbents have been reported in the literature, for instance, low adsorption capacity and high BOD, COD, and TOC values due to the release of soluble organic compounds from the untreated plant materials [19].

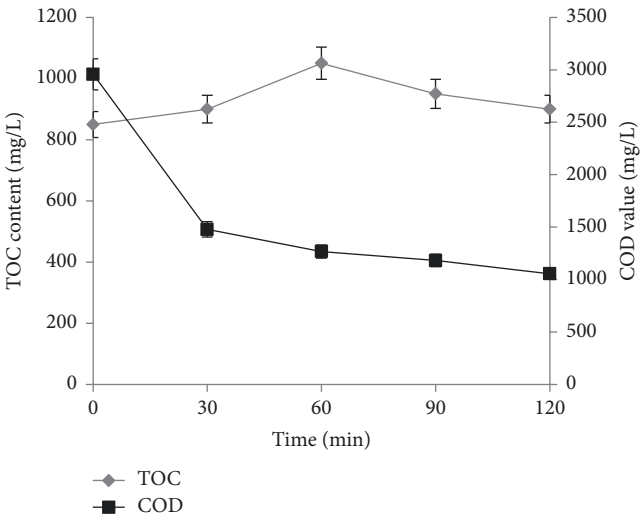

Figure 13: Profile of TOC content and COD value of treated sago wastewater under the optimised conditions during TiO_2/MSB photocatalysis (TiO_2/MSB dosage = 0.10 g; contact time = 120 min).

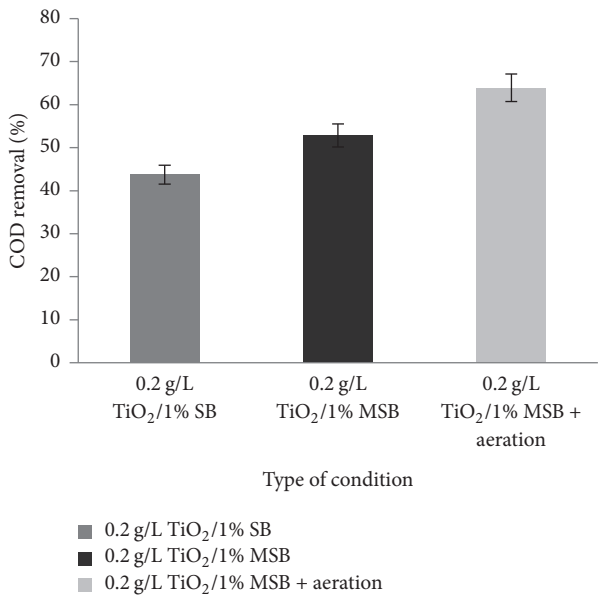

Figure 14: Efficiency of TiO_2 photocatalysis in removing COD under different conditions.

4. Conclusion

TiO_2/MSB mixture was prepared by mixing TiO_2 with the MSB. Six different TiO_2/MSB mixture samples were prepared to treat sago wastewater by varying the concentrations of TiO_2 and MSB. Maximum removal of 64.92% was achieved with an optimum loading of 0.2 g/L TiO_2/1% MSB after

120 min of irradiation. The dosage and contact time were fixed as the independent variables, while COD removal percentage was chosen as the dependent variable or response. Under the optimised RSM condition, 52.83% COD removal was attained using 0.10 g TiO_2/MSB mixture and contact time of 120 min. The efficiency of the optimised TiO_2/MSB mixture was found to be appreciably enhanced in the presence of aeration, which increased the COD removal of sago wastewater to 63.89%. Thus, based on the proposed mechanism, the efficiency of the TiO_2/MSB mixture was attributed to its dual functions, namely, the adsorption capacity of the MSB and the photocatalytic activity of TiO_2. The R^2 value of the model ($R^2 > 0.99$) depicted a high degree of correlation between the parameters. Thus, TiO_2 photocatalytic treatment can be a potential method for sago wastewater degradation using TiO_2/MSB.

Conflicts of Interest

The authors declare that there are no conflicts of interest regarding the publication of this article.

Acknowledgments

This study was supported by research grants from the Ministry of Higher Education, Malaysia, under the Research Acculturation Collaboration Effort (RACE) with Grant no. RACE/b/1245/201(01) and the Fundamental Research Grant Scheme [FRGS/SG01 (01)/1204/2014(05)]. The authors wish to thank UNIMAS for sponsoring the Zamalah Postgraduate Scholarship and the financial support, Mybrain 15 Scholarship, by the Malaysian government.

References

[1] A. R. Yazdanbakhsh, A. S. Mohammadi, M. Sardar, H. Godini, and M. Almasian, "Cod removal from synthetic wastewater containing azithromycin using combined coagulation and a fenton-like process," *Environmental Engineering and Management Journal*, vol. 13, no. 12, pp. 2929–2936, 2014.

[2] S. H. Y. S. Abdulah, M. A. A. Hassan, Z. Z. Noor, and A. Aris, "Optimization of photo-Fenton oxidation of sulfidic spent caustic by using response surface methodology," in *Proceedings of the 3rd National Postgraduate Conference - Energy and Sustainability: Exploring the Innovative Minds, NPC 2011*, Malaysia, September 2011.

[3] D. Kanakaraju, B. D. Glass, and M. Oelgemöller, "Titanium dioxide photocatalysis for pharmaceutical wastewater treatment," *Environmental Chemistry Letters*, vol. 12, no. 1, pp. 27–47, 2014.

[4] P. Kumar, S. Kumar, N. K. Bhardwaj, and S. Kumar, "Titanium dioxide photocatalysis for the pulp and paper industry wastewater treatment," *Indian Journal of Science and Technology*, vol. 4, no. 3, pp. 327–332, 2011.

[5] H. Dong, G. Zeng, L. Tang et al., "An overview on limitations of TiO_2-based particles for photocatalytic degradation of organic pollutants and the corresponding countermeasures," *Water Research*, vol. 79, pp. 128–146, 2015.

[6] A. Fujishima, X. Zhang, and D. A. Tryk, "TiO_2 photocatalysis and related surface phenomena," *Surface Science Reports*, vol. 63, no. 12, pp. 515–582, 2008.

[7] M. N. Chong, B. Jin, C. W. K. Chow, and C. Saint, "Recent developments in photocatalytic water treatment technology: a review," *Water Research*, vol. 44, no. 10, pp. 2997–3027, 2010.

[8] R. Fagan, D. E. McCormack, D. D. Dionysiou, and S. C. Pillai, "A review of solar and visible light active TiO2 photocatalysis for treating bacteria, cyanotoxins and contaminants of emerging concern," *Materials Science in Semiconductor Processing*, vol. 42, pp. 2–14, 2016.

[9] L. Giraldo and J. C. Moreno-Pirajan, "Activated carbon prepared from orange peels coated with titanium oxide nanoparticles: Characterization and applications in the decomposition of NOx," *Oriental Journal of Chemistry*, vol. 30, no. 2, pp. 451–461, 2014.

[10] S. M. Gupta and M. Tripathi, "A review of TiO_2 nanoparticles," *Chinese Science Bulletin*, vol. 56, no. 16, pp. 1639–1657, 2011.

[11] C. Ngamsopasiriskun, S. Charnsethikul, S. Thachepan, and A. Songsasen, "Removal of phenol in aqueous solution by nanocrystalline TiO_2/activated carbon composite catalyst," *Kasetsart Journal: Natural Science*, vol. 44, no. 6, pp. 1176–1182, 2010.

[12] D. S. Awg-Adeni, S. Abd-Aziz, K. Bujang, and M. A. Hassan, "Bioconversion of sago residue into value added products," *African Journal of Biotechnology*, vol. 9, no. 14, pp. 2016–2021, 2010.

[13] A. Muthukumar and M. Muthuchamy, "Contribution of ozone, pH and temperature in the inactivation of a foodborne pathogen Listeria monocytogenes- A study using response surface methodology," *International Journal on Applied Bio-Engineering*, vol. 8, no. 1, pp. 5–13, 2014.

[14] APHA, *Standard Methods for the Examination of Water and Wastewater*, 18th, Ed., America Public Health Association, Washington, Wash, USA, 1999.

[15] S. Ethaib, R. Omar, M. K. S. Mazlina, A. B. D. Radiah, and S. Syafiie, "Microwave-assisted dilute acid pretreatment and enzymatic hydrolysis of sago palm bark," *Bioresources*, vol. 11, no. 3, pp. 5687–5702, 2016.

[16] A. Kristiani, H. Abimanyu, A. H. Setiawan, Sudiyarmanto, and F. Aulia, "Effect of pretreatment process by using diluted acid to characteristic of oil palm's frond," in *Proceedings of the International Conference on Sustainable Energy Engineering and Application, ICSEEA 2012*, pp. 183–189, Indonesia, November 2012.

[17] N. Mosier, C. Wyman, B. Dale et al., "Features of promising technologies for pretreatment of lignocellulosic biomass," *Bioresource Technology*, vol. 96, no. 6, pp. 673–686, 2005.

[18] Y. Zheng, Z. Pan, and R. Zhang, "Overview of biomass pretreatment for cellulosic ethanol production," *International Journal of Agricultural and Biological Engineering*, vol. 2, no. 3, pp. 51–68, 2009.

[19] W. S. Wan Ngah and M. A. K. M. Hanafiah, "Removal of heavy metal ions from wastewater by chemically modified plant wastes as adsorbents: a review," *Bioresource Technology*, vol. 99, no. 10, pp. 3935–3948, 2008.

[20] M. A. Tony and Z. Bedri, "Experimental Design of Photo-Fenton Reactions for the Treatment of Car Wash Wastewater Effluents by Response Surface Methodological Analysis," *Advances in Environmental Chemistry*, vol. 2014, pp. 1–8, 2014.

[21] K. Yetilmezsoy, S. Demirel, and R. J. Vanderbei, "Response surface modeling of Pb(II) removal from aqueous solution by Pistacia vera L.: Box-Behnken experimental design," *Journal of Hazardous Materials*, vol. 171, no. 1-3, pp. 551–562, 2009.

[22] V. Sangeetha, V. Sivakumar, A. Sudha, and K. S. Priyenka Devi, "Optimization of process parameters for COD removal by coagulation treatment using box-behnken design," *International Journal of Engineering and Technology*, vol. 6, no. 2, pp. 1053–1058, 2014.

[23] D. A. D. A. Aljuboury, P. Palaniandy, H. B. A. Aziz, and S. Feroz, "Evaluation of the solar photo-Fenton process to treat the petroleum wastewater by response surface methodology (RSM)," *Environmental Earth Sciences*, vol. 75, no. 4, article no. 333, pp. 1–12, 2016.

[24] A. Kumar, B. Prasad, and I. M. Mishra, "Process parametric study for ethene carboxylic acid removal onto powder activated carbon using Box-Behnken design," *Chemical Engineering & Technology*, vol. 30, no. 7, pp. 932–937, 2007.

[25] I. Arslan-Alaton, G. Tureli, and T. Olmez-Hanci, "Treatment of azo dye production wastewaters using Photo-Fenton-like advanced oxidation processes: Optimization by response surface methodology," *Journal of Photochemistry and Photobiology A: Chemistry*, vol. 202, no. 2-3, pp. 142–153, 2009.

[26] F.-S. Zhang and H. Itoh, "Photocatalytic oxidation and removal of arsenite from water using slag-iron oxide-TiO2 adsorbent," *Chemosphere*, vol. 65, no. 1, pp. 125–131, 2006.

[27] G. Wang, L. Xu, J. Zhang, T. Yin, and D. Han, "Enhanced photocatalytic activity of TiO_2 powders (P25) via calcination treatment," *International Journal of Photoenergy*, vol. 2012, Article ID 265760, 2012.

[28] K. Sathasivam and M. R. H. Mas Haris, "Adsorption kinetics and capacity of fatty acid-modified banana trunk fibers for oil in water," *Water, Air, & Soil Pollution*, vol. 213, no. 1-4, pp. 413–423, 2010.

[29] S. Vitolina, G. Shulga, B. Neiberte et al., "The efficiency of biomass removal from model woodworking wastewater with polyethylenimine," in *Proceedings of the The 9th International Conference "Environmental Engineering 2014"*, Vilnius, Lithuania, May 2014.

[30] G. Hegde, S. A. Abdul Manaf, A. Kumar et al., "Biowaste Sago Bark Based Catalyst Free Carbon Nanospheres: Waste to Wealth Approach," *ACS Sustainable Chemistry & Engineering*, vol. 3, no. 9, pp. 2247–2253, 2015.

[31] D. Kanakaraju, S. Ravichandar, and Y. C. Lim, "Combined effects of adsorption and photocatalysis by hybrid TiO2/ZnO-calcium alginate beads for the removal of copper," *Journal of Environmental Sciences*, vol. 55, pp. 214–223, 2017.

[32] M. M. Abou-Sekkina, M. A. Sakran, and A. A. Saafan, "Development of correlations among the spectral, structural, and electrical properties and chemical treatment of Egyptian cotton fabric strips," *Industrial & Engineering Chemistry Product Research and Development*, vol. 25, no. 4, pp. 676–680, 1986.

[33] O. Carp, C. L. Huisman, and A. Reller, "Photoinduced reactivity of titanium dioxide," *Progress in Solid State Chemistry*, vol. 32, no. 1-2, pp. 33–177, 2004.

[34] P. R. Gogate and A. B. Pandit, "A review of imperative technologies for wastewater treatment I: oxidation technologies at ambient conditions," *Advances in Environmental Research*, vol. 8, no. 3-4, pp. 501–551, 2004.

[35] U. I. Gaya and A. H. Abdullah, "Heterogeneous photocatalytic degradation of organic contaminants over titanium dioxide: a review of fundamentals, progress and problems," *Journal of Photochemistry and Photobiology C: Photochemistry Reviews*, vol. 9, no. 1, pp. 1–12, 2008.

[36] G. Li Puma, A. Bono, and J. G. Collin, "Preparation of titanium dioxide photocatalyst loaded onto activated carbon support using chemical vapor deposition: A review paper," *Journal of Hazardous Materials*, vol. 157, no. 2-3, pp. 209–219, 2008.

[37] Y. Liu, S. Yang, J. Hong, and C. Sun, "Low-temperature preparation and microwave photocatalytic activity study of TiO_2-mounted activated carbon," *Journal of Hazardous Materials*, vol. 142, no. 1-2, pp. 208–215, 2007.

[38] F. Xu, G. Cheng, S. Song, Y. Wei, and R. Chen, "Insights into Promoted Adsorption Capability of Layered BiOCl Nanostructures Decorated with TiO_2 Nanoparticles," *ACS Sustainable Chemistry & Engineering*, vol. 4, no. 12, pp. 7013–7022, 2016.

[39] M. Kumar, F. I. A. Ponselvan, J. R. Malviya, V. C. Srivastava, and I. D. Mall, "Treatment of bio-digester effluent by electrocoagulation using iron electrodes," *Journal of Hazardous Materials*, vol. 165, no. 1-3, pp. 345–352, 2009.

[40] M. Hadavifar, A. A. Zinatizadeh, H. Younesi, and M. Galehdar, "Fenton and photo-Fenton treatment of distillery effluent and optimization of treatment conditions with response surface methodology," *Asia-Pacific Journal of Chemical Engineering*, vol. 5, no. 3, pp. 454–464, 2010.

[41] R. L. Mason, R. F. Gunst, and J. L. Hess, *Statistical design and analysis of experiments*, Wiley Series in Probability and Statistics, Wiley-Interscience [John Wiley & Sons], USA, Hoboken, NJ, USA, 2nd edition, 2003.

[42] B. Sadler, *Light metals 2013*, John Wiley Sons, Hoboken, NJ, USA, 2013.

[43] J. C. Costa and M. M. Alves, "Posttreatment of olive mill wastewater by immobilized TiO_2 photocatalysis," *Photochemistry and Photobiology*, vol. 89, no. 3, pp. 545–551, 2013.

[44] D. A. D. A. Aljuboury, P. Palaniandy, H. B. A. Aziz, S. Feroz, and S. S. A. Amr, "Evaluating photo-degradation of COD and TOC in petroleum refinery wastewater by using TiO_2/ZnO photocatalyst," *Water Science and Technology*, vol. 74, no. 6, pp. 1312–1325, 2016.

[45] S. Yao, J. Li, and Z. Shi, "Immobilization of TiO_2 nanoparticles on activated carbon fiber and its photodegradation performance for organic pollutants," *Particuology*, vol. 8, no. 3, pp. 272–278, 2010.

[46] A. Omri and M. Benzina, "Almond shell activated carbon: adsorbent and catalytic support in the phenol degradation," *Environmental Modeling & Assessment*, vol. 186, no. 6, pp. 3875–3890, 2014.

[47] D. a. Aljuboury, P. Palaniandy, H. B. Abdul Aziz, and S. Feroz, "Evaluating the TiO_2 as a solar photocatalyst process by response surface methodology to treat the petroleum waste water," *Karbala International Journal of Modern Science*, vol. 1, no. 2, pp. 78–85, 2015.

[48] D. Kanakaraju, C. A. Motti, B. D. Glass, and M. Oelgemöller, "Solar photolysis versus TiO_2-mediated solar photocatalysis: a kinetic study of the degradation of naproxen and diclofenac in various water matrices," *Environmental Science and Pollution Research*, vol. 23, no. 17, pp. 17437–17448, 2016.

[49] Department of Environment (DOE), *Environmental Requirements: A Guide for Investor*, Environmental Requirements: A Guide for Investor, Putrajaya, Malaysia, 11th edition, 2010.

[50] M. Yasmina, K. Mourad, S. H. Mohammed, and C. Khaoula, "Treatment heterogeneous photocatalysis; Factors influencing the photocatalytic degradation by TiO_2," in *Proceedings of the International Conference on Technologies and Materials for Renewable Energy, Environment and Sustainability, TMREES 2014 - EUMISD*, pp. 559–566, Lebanon, April 2014.

[51] S. Malato, P. Fernández-Ibáñez, M. I. Maldonado, J. Blanco, and W. Gernjak, "Decontamination and disinfection of water by solar photocatalysis: recent overview and trends," *Catalysis Today*, vol. 147, no. 1, pp. 1–59, 2009.

[52] P. A. Pekakis, N. P. Xekoukoulotakis, and D. Mantzavinos, "Treatment of textile dyehouse wastewater by TiO_2 photocatalysis," *Water Research*, vol. 40, no. 6, pp. 1276–1286, 2006.

[53] F. N. Acar and Z. Eren, "Removal of Cu(II) ions by activated poplar sawdust (Samsun Clone) from aqueous solutions," *Journal of Hazardous Materials*, vol. 137, no. 2, pp. 909–914, 2006.

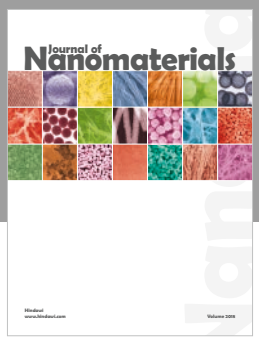

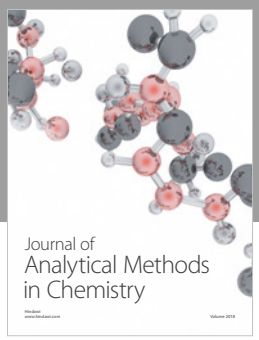

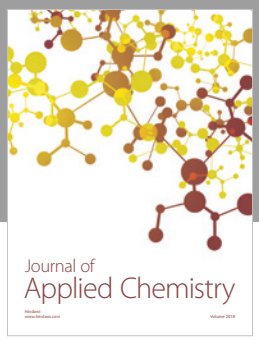

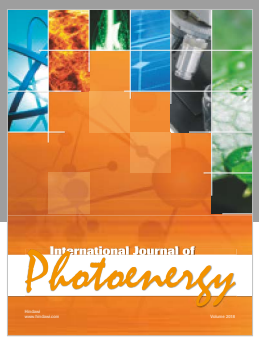

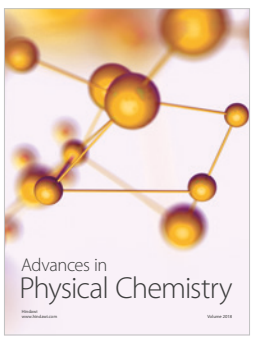

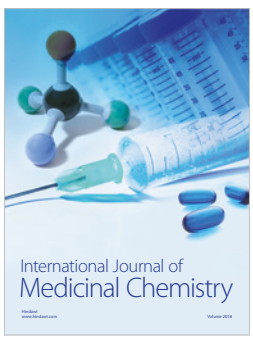

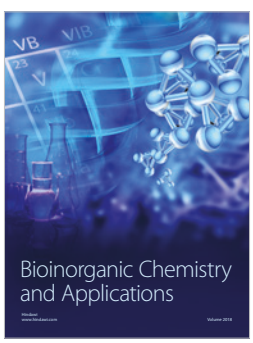

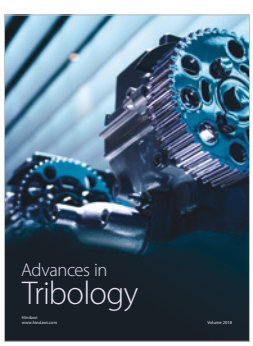

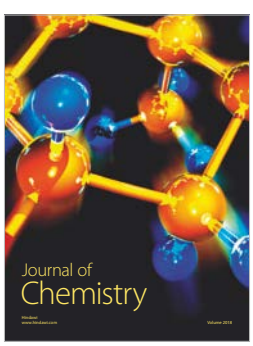

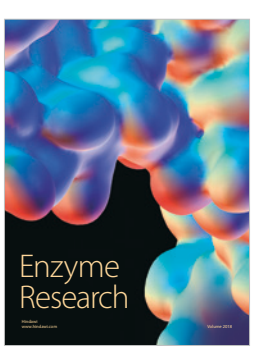

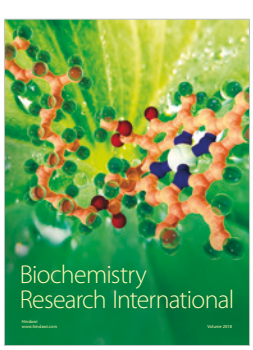

Hindawi

Submit your manuscripts at
www.hindawi.com